# Vehicle Health Monitoring System using Multiple-Model Adaptive Estimation

Xudong Wang, Martian Binonwangan, and Vasillis Syrmos
Department of Electrical Engineering
University of Hawaii at Manoa
Honolulu, HI 96822
hellas@euclid.eng.hawaii.edu

***Abstract*— In this paper, we propose Multiple-Models Adaptive Estimation (MMAE) for Failure Detection and Identification (FDI) of aircraft components, i.e, flaps, landing gears. The MMAE FDI consists of parallel Kalman filters and each Kalman filter is constructed to represent a specific failure mode including the nominal mode. The Kalman filter residuals are post processed to produce the log-likelihood function values using sliding window methods, and posterior probabilities. The hypothesis with the maximum log-likelihood function values is declared the most possible mode of the system at the current decision time, and the probability-weighted average state estimate $(\hat{x}_{MMAE})$ is calculated. We apply this method to the DC motor system, and evaluate the performance with sensors failures. Simulation results show that the MMAE is simple to implement and effective in fault detection and identification.**

***Index Terms*—Kalman filter, Sliding window, Failure Detection and Identification**

## I. Introduction

MODERN engineering systems are becoming more and more sophisticated. Reliability, availability, and automatic supervision of technical processes and their control systems are important consideration in overall system design and operation. An integral element of a highly reliable, fault-tolerant system is an efficient fault detection and identification technique that can detect and isolate the sensors, actuators, or system component failures so that remedies can be undertaken. A failure is defined to be any deviation of a system from its normal or intended behavior; diagnosis is the process of detecting an abnormality in the system behavior and isolating the cause or the source of this abnormality. Hard failure can be rapidly detected by on-line built-in-testing (BIT), the more subtle or "soft" drifting-type failures can only be detected by the use of more sophisticated techniques, based on modern estimation/decision theory [1]. Towards this, many methods have been developed for fault detection and identification of dynamics systems over the last two decades [2, 3, 4, 5, 6].

In a modern flight control system, for example, failures of its actuator or sensor may cause serious problems and need to be detected and identified as soon and as accurately as possible. Systems subject to such failures cannot be modelled well by a single set of equations of state that varies continuously. A more appropriate mathematical model for such a system is the so-called stochastic hybrid system. It differs from the conventional stochastic systems in that its state may jump as well as vary continuously.

One of the most effective approaches for fault detection and identification is based on the use of multiple models $(\theta_k; k = 1, 2, \ldots, M)$ which runs a bank of parallel Kalman filters, each based on a model matching to a particular model of the system, and a hypothesis testing algorithm as shown in Figure 1. The Kalman filters are provided a measurement vector and the input vector, and produce state estimates and residuals. The hypothesis-testing algorithm uses the residual to compute conditional likelihood function of the various hypotheses that are modelled in the Kalman filters, conditioned on the history of the measurements received up to that time, and make the failure/ no failure decision and isolate the failure modes. The hypothesis-testing algorithm can also assign conditional probabilities to each of the hypotheses that are used to form the Kalman filter models. Theses conditional probabilities indicate the relative correctness of the various filter models, and can be used to probability-weighted average state estimate $(\hat{x}_{MMAE})$.

The remaining parts of the paper are organized as follows. Section 2 describes the Kalman filter based on the true system, the hypothesis modes and the hypothesis-testing algorithm. Section 3 presents the simulation results based on the pre-assumed failure sequence. Section 4 discusses the multiple-hypothesis failure detection and identification approaches.

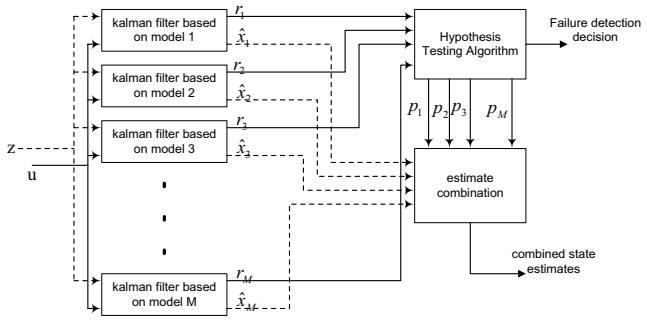


Fig. 1. MMAE Algorithm

This research has been funded by The Boeing Company under contract # 436481.

## II. System model

In the multiple models method, a set of models is assumed to represent the possible system behavior patterns or structures (system modes); a bank of Kalman filters runs in parallel at every time, each based on a particular model, to obtain model-based estimates and check the status of the operation system; the overall state estimate is a kind of combination of those model-based estimates.

### A. Multiple Model Adaptive Estimation Equations

*1) Basic Kalman Filter Equations:* We assume a steady state Kalman filter model associated with a particular hypothesized mode with the subscript k.

$$x_k(t_i) = \Phi_k x_k(t_{i-1)} + B_k u(t_{i-1}) + w_k(t_i) \quad (1)$$

$$z_k(t_i) = H_k x_k(t_i) + v_k(t_i) \quad (2)$$

where

$x_k$ is the state vector,

$\Phi_k$ is the state transition matrix,

$B_k$ is the control input matrix,

$u_k$ is the system input vector,

$w_k$ is an additive white Gaussian processing noise with zero mean and covariance as:

$$E\left[w_k(t_i)w_k^T(t_j)\right] = Q_k\delta_{ij} \quad (3)$$

$z_k$ is the measurement vector,

$H_k$ is the measurement matrix,

$v_k$ is an additive white Gaussian measurement noise input with zero mean and variance

$$E\left[v_k(t_i)v_k^T(t_j)\right] = R_k\delta_{ij} \quad (4)$$

The measurement noise sequence $v_k(t_i)$ and processing noise sequence $w_k(t_j)$ are independent of each other.

The Kalman filter algorithm uses the above model to define time propagation and measurement update equations of the Kalman filter state estimates and state estimate covariance matrix. The Kalman filter state estimate propagation equation is:

$$\hat{x}_k(t_i^-) = \Phi_k\hat{x}_k(t_{i-1}^+) + B_k u(t_{i-1}) \quad (5)$$

$$\hat{z}_k(t_i^-) = H_k\hat{x}(t_i^-) \quad (6)$$

where

$\hat{x}_k(t_i^-)$ is the state estimate before the measurement vector is available,

$\hat{z}_k(t_i^-)$ is the estimate of the measurement vector before it becomes available, and the state estimate covariance matrix propagation equation

$$P_k(t_i^-) = \Phi_k P_k(t_{i-1}^+)\Phi_k^T + Q_k \quad (7)$$

and when the measurement vector at $t_i$ is available, the state estimates are updated as:

$$\hat{x}_k(t_i^+) = \hat{x}_k(t_i^-) + K_k(t_i)(z_k(t_i) - H_k\hat{x}_k(t_i^-)) \quad (8)$$

where the Kalman filter gain is

$$K_k(t_i) = P_k(t_i^-)H_k^T\left[H_k P_k(t_i^-)H_k^T + R_k\right]^{-1} \quad (9)$$

The Kalman filter residual vector is defined as

$$r_k(t_i) = z_k(t_i) - H_k\hat{x}_k(t_i^-) \quad (10)$$

which is the difference between the measurements and the Kalman filter estimates based on its model. Finally, the Kalman filter state estimate covariance matrix is updated using

$$P_k(t_i^+) = P_k(t_i^-) - K_k(t_i)H_k P_k(t_i^-) \quad (11)$$

The steady state of the Kalman filter estimate of the state covariance matrix can be pre-computed by iterating (7), (9) and (11) until steady state of the covariance and gain matrices is reached. With the steady state implementation, the state covariance matrix, the steady state Kalman filter gain, and the steady Kalman filter residual covariance matrices therefore don't need to be computed in real time. The steady state Kalman filter can be

$$\hat{x}_k(t_i^-) = \Phi_k\hat{x}_k(t_{i-1}^+) + B_k u(t_{i-1}) \quad (12)$$

for the state estimates propagation and

$$\hat{x}_k(t_i^+) = \hat{x}_k(t_i^-) + K_k(t_i)r_k(t_i) \quad (13)$$

for updating the state estimates.

*2) Hypothesis Testing Algorithm:* The residual sequence has been shown to be a white Gaussian sequence of mean zero and covariance $[H_k P_k(t_i^-)H_k^T + R_k]$. This can be exploited for the practical purpose of either sensor failure detection or reasonableness checking of measurement data [7].

Optimal "likelihood function" methods can be used to perform a test for the occurrence of a sensor failure. Essentially the $N$ most recent residual signals are investigated to determine whether they differ significantly from the statistical description of their values that assumes no failures. The number $N$ is a design parameter. In common sense, it is kept to be greater than one to prevent failure declarations because consistently large residuals indicate abnormalities, whereas individual realization of large magnitude is to be expected. On the other hand, it is not appropriate to use all the residuals from the initial time to current time, since this would smooth the sensitivity to true failures as time progressed. Thus, we use a "sliding window" of the $N$ most recent samples, and the $N$ is on the order of 5 to 20. Statistical hypothesis testing theory indicated that a good choice of likelihood function for event of failure detection would be in the form of sum of natural logs of conditional densities for components of residuals: for the $k^{th}$ component

$$L_{N_k}(t_i) = \sum_{j=i-N+1}^{i} ln(f_{r_k(t_j)|r_k(t_{j-1})\ldots r_k(t_1)}(\rho_j|\rho_{j-1}\cdots\rho_1)) \quad (14)$$

Since the residual sequence can be assumed to be a set of independent zero-mean Gaussian random variable, the above likelihood function can be written as:

$$L_{N_k}(t_i) = -0.5\sum_{j=i-N+1}^{i}[r_k^T(t_j)A_k^{-1}r_k(t_j) + log|A_k|] \quad (15)$$

where

$$A_k = H_k P_k(t_i^-)H_k^T + R_k \quad (16)$$

In (15), we calculate the $L_N(t_i)$ values for each hypothesis model, and pick the maximum one which would represent the most possible operation status of the system.

*3) Posterior probabilities and combined state estimates:* Since the Kalman filter residual is a white Gaussian sequence of mean zero and covariance as (16), we can get the conditional density function of the measurement $z$ at $t_i$ for the $k^{th}$ hypothesis model, conditioned on the measurement history up to time $t_{i-1}$, $Z(t_{i-1}) = \{z(t_1), \ldots, z(t_{i-1})\}$

$$f_{z(t_i)|\theta, Z(t_{i-1})}(z_i|\theta_k, Z_{i-1}) = \beta exp\{.\} \tag{17}$$

where

$$\beta = \frac{1}{(2\pi)^{m/2}|A_k|^{1/2}} \tag{18}$$

$$\{.\} = \{-\frac{1}{2} r_k^T(t_i) A_k^{-1} r_k(t_i)\} \tag{19}$$

We can define the conditional probability for a particular hypothesis model as:

$$p_k(t_i) = Pr(\theta = \theta_k | Z(t_i) = Z_i) \tag{20}$$

In [8], the conditional probability of $k^{th}$ hypothesis model is updated as:

$$p_k(t_i) = \frac{f_{z(t_i)|\theta, Z(t_{i-1})} p_k(t_{i-1})}{\sum_{j=1}^{M} f_{z(t_i)|\theta, Z(t_{i-1})} p_j(t_{i-1})} \tag{21}$$

Here, we use the prior conditional probabilities, $p_k(t_{i-1})$ to compute the conditional probabilities on the current measurement. For fault detection and identification problem, we can also use the conditional probabilities of the hypothesis models to detect the abnormality of the system. As we stated in the introduction part, we are going to use the conditional probabilities to weight and blend the various hypothesis, and get the $\hat{x}_{MMAE}$ as:

$$\hat{x}_{MMAE} = \sum_j \hat{x}_j(t_i) p_j(t_i) \tag{22}$$

where $\hat{x}_j(t_i)$ is the $j^{th}$ Kalman filter state estimate.

### B. System failure modes

In this paper, system failure modes are focused on the $\Phi$, $B$ and $H$ variations because they are the most common failure scenarios in the complex system. When we design the Kalman filter bank, we assumed that the Kalman filter model and the true model are of the same dimension and that the dynamics noise strength $Q$, measurement noise strength $R$ are equivalent.

In the failure detection and identification of the aircraft flight control system, the actuator failure can be modelled as:

$$x_k(t_i) = \Phi_k x_k(t_{i-1}) + (B_k + M_j) u(t_{i-1}) + w_k(t_{i-1}) \tag{23}$$

That is to choose the matrix $M_j$ with all zero elements except that the $j^{th}$ column is taken to the negative of the $j^{th}$ element of input matrix $B_k$.

For the sensor failure, we have two situations:

*1) Partial sensor failure:* Partial sensor failure can be modelled by increasing the measurement noise covariance matrix $R$.

*2) Total sensor failure:* For the total sensor failure, a similar idea can be followed, the failures can be modelled by annihilating the appropriate row of the measurement matrix $H$ as:

$$z_k(t_i) = (H_k + L_j) x_k(t_i) + v_k(t_i) \tag{24}$$

Here we consider combination of the partial and total sensor failures, and simultaneous failures of the different sensors. These situations require that failure detection and identification algorithm to be more responsive and robust.

### C. Physical models

Different measurable signals can be used to evaluate the response of the DC motor that can be applied to control the motion of the aircraft flap. Measurable signals can be the angular position and velocity of the motor shaft, voltage and current at the terminal of the motors. For simplicity, we measure the angular position and velocity of the shaft and the sensors used are gyroscope and incremental encoder [9].

*1) Gyroscope:* The gyroscope measurement can be modelled as:

$$\omega_g = \omega + b + v_g \tag{25}$$

where $\omega$ is the true angular velocity of the shaft, $v_g$ is additive white Gaussian noise with zero mean and certain covariance, and $b$ is gyroscope bias drift term which can be modelled as random walk:

$$\frac{db}{dt} = n_b \tag{26}$$

where $n_b$ is assumed to be zero-mean Gaussian with known variance. The gyroscope measurement is assumed to be available at the kalman filter update rate of 0.005 seconds.

*2) Incremental Encoder:* The incremental encoder can be modelled as:

$$\theta_e = \theta + v_e \tag{27}$$

where $\theta$ is the true angular position of the shaft of the motor and $v_e$ is assumed to be zero-mean Gaussian with known variance. The encoder measurement is updated every 0.05 seconds.

*3) DC Motor Model:* The dynamics of a DC servo motor are described by the electrical signals and the mechanical motion of the armature as follows:

$$L_a \frac{di_a}{dt} + R_a i_a = v_a - K_e \dot{\theta} \tag{28}$$

$$J\ddot{\theta} + b\dot{\theta} = K_t i_a \tag{29}$$

where the description of the symbols are enumerated in Table I.

*4) Integrated Model:* Combining (25), (26), (27), (28), and (29), a continuous state-space model can be formulated as:

$$\dot{x} = \Phi x + Bu + G n_b \tag{30}$$

where $x = \begin{pmatrix} \dot{\theta} \\ \dot{\omega} \\ \dot{i} \\ \dot{b} \end{pmatrix}$, $B = \begin{pmatrix} 0 & 0 \\ 0 & -\frac{N}{J} \\ \frac{1}{L_a} & 0 \\ 0 & 0 \end{pmatrix}$, $G = \begin{pmatrix} 0 \\ 0 \\ 0 \\ 1 \end{pmatrix}$,

$u = \begin{pmatrix} v_a \\ T_L \end{pmatrix}$, and $\Phi = \begin{pmatrix} 0 & \frac{1}{N} & 0 & 0 \\ 0 & -\frac{b}{J} & \frac{N^2 K_t}{J} & 0 \\ 0 & -\frac{K_e}{L_a} & -\frac{R_a}{L_a} & 0 \\ 0 & 0 & 0 & 0 \end{pmatrix}$.

TABLE I

MOTOR MODEL PARAMETERS

| Symbol | Description |
|---|---|
| $J$ | Moment of inertia of motor and load |
| $b$ | Viscous damping of motor and load |
| $L_a$ | Inductance of the armature |
| $R_a$ | Resistance of the armature |
| $v_a$ | Voltage across the terminal |
| $K_e$ | Back EMF |
| $K_t$ | Torque sensitivity |
| $N$ | Gear Raio |

The corresponding output equation is:

$$z(t) = \begin{pmatrix} 1 & 0 & 0 & 0 \\ 0 & 1 & 0 & 1 \end{pmatrix} \begin{pmatrix} \theta \\ \omega \\ i \\ b \end{pmatrix} + \begin{pmatrix} v_e \\ v_g \end{pmatrix}$$

## III. SIMULATION RESULTS

Figure 2 depicts the failure scenario assumed during the operation of the DC motor. Each of the failures is explained in detail below:

- $H0$ *Nominal operation* – All systems are functioning properly. The nominal parameters used for the Kalman filter are representative of the actual system.
- $H1$ *Noisy Gyro* – All the systems except the gyroscope are functioning properly. Soft failure of the gyroscope is simulated as the increase in the gyroscope measurement noise. The covariance of the noise of the gyroscope is increased by 100 times larger than the nominal value.
- $H2$ *Noisy Gyro* – Similar scenario as $H1$ but the noise of the gyroscope is increased by 500 times larger than the nominal value.
- $H3$ *Failed Gyro* – All systems except the gyroscope are functioning properly. The gyroscope completely fails during service (Hard failure). It is not participating in measuring the response of the motor; it is only outputting signal composed of random noise.
- $H4$ *Noisy encoder* – All the systems except incremental encoder is functioning properly. Soft failure of the incremental encoder is simulated as the increase in the variance of the measurement noise of 100 times larger than the nominal value.
- $H5$ *Failed Encoder* – All the systems except the incremental encoder are functioning properly. Hard failure of the encoder is being experienced. The encoder is generating random noise as its output signal.

Because of the difference in the sampling rates between the gyro and the incremental encoder, two parallel sets of multiple hypothesis Kalman filters are used: $MH-KF^I$ includes gyro failures, while $MH-KF^{II}$ includes incremental encoder failures. $MH-KF^I$ uses the models: $H0$ nominal operation, $H1$ increased gyro noise 1, $H2$ increased gyro noise 2, $H3$ gyro dropout, and $MH-KF^{II}$ with $H0$ nominal operation, $H4$ increased encoder noise, and $H5$ encoder dropout. Each setup of the Kalman filter based on the corresponding hypothesis, and Q, R and H parameters are chosen to represent the corresponding hypothesis.

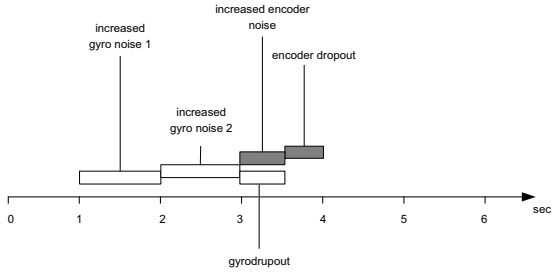


Fig. 2. Failure sequence used for FDI simulation

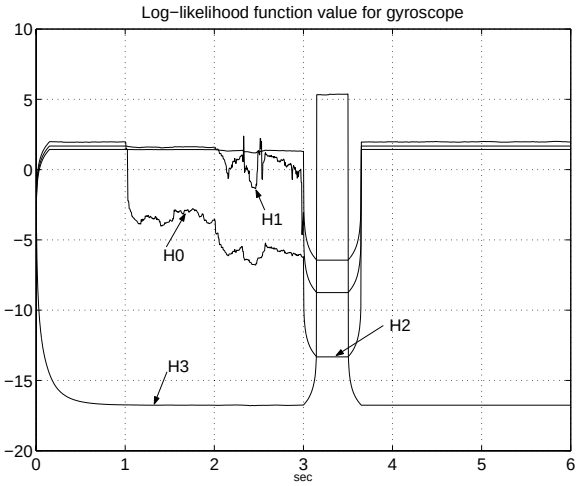


Fig. 3. Log-likelihood values for gyro hypothesis models

In Figure 3, it is clear that the log-likelihood value for $H0$ (nominal operation) changed at $t = 1$ seconds, and $H1$, $H2$ and $H3$ become the likely operation status of the gyroscope. For example, by comparing the evolution of log-likelihood values for gyroscope, we can conclude that the log-likelihood value for $H3$ hypothesis becomes dominant after $t = 3$ seconds, thus the $H3$ (Failed Gyro) is the most likely from $t = 3$ seconds. It is noticeable that there exists some lag for the detection of $H3$ comparing with the failure scenario in Figure 2. The reason for this lag is due to the sliding window, it can be shortened if the likelihood calculation can be done over shorter sliding windows in the condition of the assumed fault-tolerant. Similar results can be obtained for the evolution of operation status of the incremental encoder in Figure 4.

Analysis of the posterior probabilities of the hypothesis for the $MH-KF^I$ and $MH-KF^{II}$ clearly shows five failure periods in Figures 5 and 6. Posterior probabilities corresponding to the different hypothesis ($H0$, $H1$, $H2$, $H3$, $H4$, and $H5$) indicate when the gyro or incremental encoder is going to suffer the failures (represented by 0-1 and 1-0 switching). Furthermore, failures are identified unambiguously and almost instantaneously. The attractiveness of the posterior probabilities is that we can weigh the state estimates from the entire hypothesis models to produce the combined current state estimate as

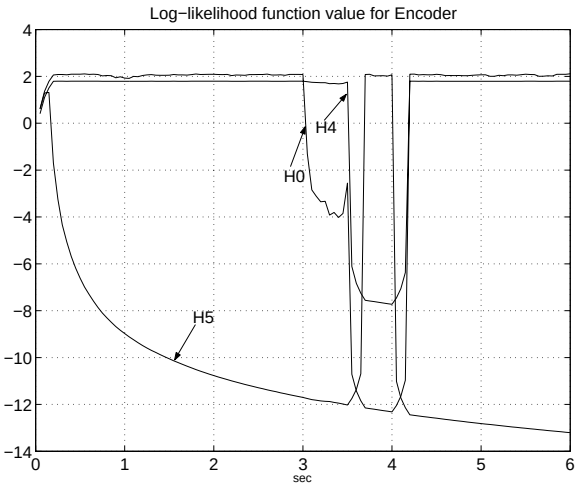


Fig. 4. Log-likelihood values for encoder hypothesis models

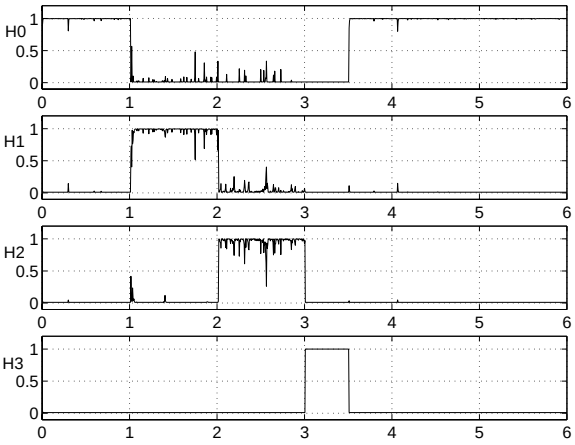


Fig. 5. Posterior probabilities: $MH - KF^I$

shown in Figure 7.

## IV. Conclusion

The multiple model estimation technique, such as multiple hypothesis kalman filters, can detect and identify the failure of gyroscope and incremental encoder with the proper testing algorithm, such as log-likelihood function with the proper sliding window size. A common problem encountered with the multi-hypothesis Kalman filter is the delay in detection due to build up of the likelihood function for active hypothesis. By testing the evolution of the posterior probability of each hypothesis, we can detect and identify the failure almost instantaneously, and get the probability-weighted average state estimate, $\hat{x}_{MMAE}$.

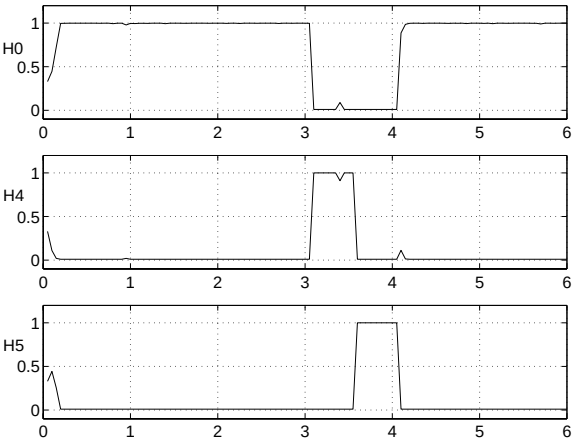


Fig. 6. Posterior probabilities: $MH - KF^{II}$

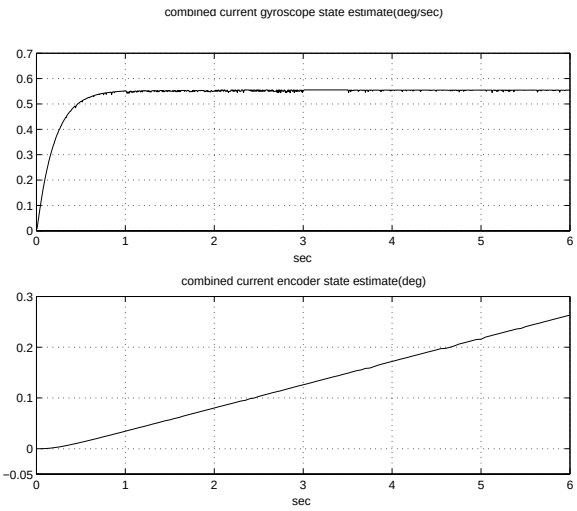


Fig. 7. Combined state estimates

## References


[1] Ali Zolghadri, *An algorithm for real time failure detection in kalman filters*, IEEE Transactions on Automatic Control, Vol. 41, No. 10, 1996, pp.1537-1539.

[2] A. Willsky, *A survey of Design Methods for Failure Detection in dynamic systems*, Automatica., Nov. 1976, pp. 601-611.

[3] R. Mehra, and J. Peschon, *An innovation approach to fault detection and diagnosis in dynamic systems*, Automatica, 7:637-640, Pergamon Press, 1971.

[4] R. Mehra, C. Rago, and S. Seereeram, *Autonomous failure detection, identification and fault-tolerant estimation with aerospace application*, IEEE Aerospace Conference Proceeding, Vol. 2, 1998.

[5] Zhang, Y. M., and Li, X. R., *Detection and diagnosis of sensor and actuator failures using IMM estimator*, IEEE Transactions on Aerospace and Electronic Systems, Vol 34, No. 4, 1998, pp. 1293-1313.

[6] Hanlon, P. D., and Maybeck, P. S., *Multiple-Model Adaptive Estimation using a residual correlation Kalman filter bank*, IEEE Transactions on Aerospace and Electronic Systems, Vol 36, No. 2, 2000, pp. 393-406.

[7] Maybeck, P. S., *Stochastic Models, Estimation and Control, Vol. 1*, New York: Academic Press, 1979.

[8] Li, X. R., and BarShalom, Y., *Multiple-model estimation with variable structure*, IEEE Transactions on Automatic Control, 41, 4, 1996, pp. 393-406.

[9] Syrmos Vassilis, *Vehicle Health monitoring system failure detection and identification*, Technical report.